Dynamic Interaction Study on Double-Pantograph and Rigid-Catenary for AC Traction Power Supply System

Qiang Huang[1(✉)], Ying Wang[1,2], Xiaoqiang Chen[1,2], Yuting Wang[1], and Jianlong Guo[1]

[1] Lanzhou Jiaotong University, Lanzhou 730070, China
hqljdlt@163.com
[2] Key Laboratory of Opto-Technology and Intelligent Control Ministry of Education, Lanzhou 730070, China

Abstract. With the development of urban rail transit and the installation of rigid catenary in low clearance tunnels during electrification renovations, the dynamic coupling of pantograph catenary in AC rigid contact network system has become a new hot topic. This article studies the coupling characteristics of the pantograph catenary under the operating conditions of dual pantographs. Equivalent AC rigid contact network to Euler Bernoulli beam based on beam theory, the pantograph model is established using three mass blocks, and the dual pantograph catenary model is established using penalty functions. The results show that under the operating condition of the AC rigid catenary, the train speed is inversely proportional to the span of the AC rigid catenary; Among the commonly used spans, a span of 8 or 10 m is suitable for train speeds below 80 km/h, while a span of 6 or 8 m is suitable for train speeds of 80–140 km/h.

Keywords: AC rigid catenary · Train · Span · Beam · Penalty function · Dual pantograph catenary

1 Introduction

In recent years, railways have developed rapidly around the world, especially with the astonishing speed of China's high-speed rail development, improving the interaction between pantograph and catenary is the key problem for train speed increase [1]. China has a vast terrain, complex landform, and more complex train operation environment, pantograph-catenary is considered the most vulnerable link in the railway traction power system [2], therefore, the research on pantograph-catenary interaction is more necessary. When the pantograph catenary interaction occurs, the catenary will fluctuate [3], further worsening the coupling performance of the pantograph catenary, at the same time, the vehicle track excitation is also one of the normal disturbances of the pantograph catenary interaction [4], and when the train passes the bridge, the vibration of the portal structure can also disturb the pantograph catenary interaction [5]. As shown in Fig. 1, the rigid

M. Gong et al. (Eds.): EITRT 2023, LNEE 1138, pp. 1–8, 2024.
https://doi.org/10.1007/978-981-99-9319-2_1

catenary is one of the catenary types, it has small installation space and low tunnel headroom. At present, DC rigid catenary is widely used in urban in China, and gradually used in railway tunnels [6].

Although AC rigid catenary are gradually being applied in China's railway, the main problems of AC rigid catenary have not yet been widely studied, the existing research mainly focuses on modeling, wear analysis, and modification of rigid catenary. A mathematical model of rigid catenary based on absolute node coordinate formula has been established to simulate the dynamic behavior of pantograph-catenary during high-speed operation in [7]. A rigid catenary pantograph-catenary coupling model considering overlapping areas was established in [8]. A pantograph-catenary coupling algorithm was established for the rigid catenary and the multi body connecting rod form of the pantograph in [9].

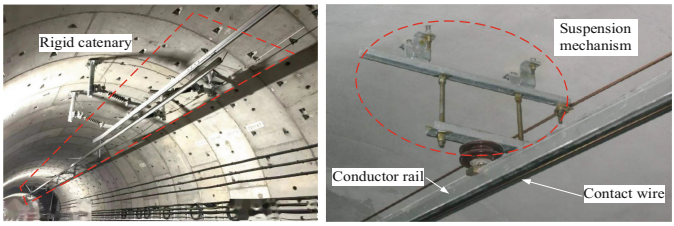

Fig. 1. Rigid catenary system

2 Double Pantograph Catenary Modeling

Based on beam theory, a vibration differential equation was established, and a double pantograph catenary model of AC rigid catenary was established.

2.1 Suspension Mechanism Modeling

As shown in Fig. 2. The suspension mechanism of the rigid contact network is mainly composed of T-bolts, suspension channel steel, insulators, positioning wire clips, $\prod$ converters and contact wires. The $\prod$ converters are fixed to the suspension channel steel by positioning wire clips and insulators, and the suspension channel steel is mounted on the tunnel wall by T-bolts.

The suspension mechanism is equivalent to a spring, with an equivalent mass of m_{eq} = 25.68kg and an equivalent stiffness of $k_{eq} = 3.78 \times 10^7$ N/m.

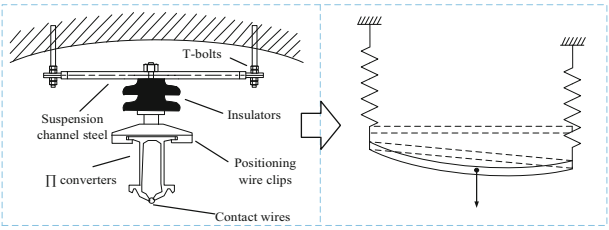

Fig. 2. Model of ∏ suspension mechanism

2.2 Double Pantograph Modeling

For the pantograph dynamic simulation model, the widely used three mass model is used, as shown in Fig. 3, m_i, k_i, c_i ($i = 1,2,3$) denote the equivalent mass, the equivalent stiffness and the equivalent damping:

$$\mathbf{M} = \begin{bmatrix} m_1 & 0 & 0 \\ 0 & m_2 & 0 \\ 0 & 0 & m_3 \end{bmatrix}$$

$$\mathbf{C} = \begin{bmatrix} c_1 & -c_1 & 0 \\ -c_1 & c_1 + c_2 & -c_2 \\ 0 & -c_2 & c_2 + c_3 \end{bmatrix} \tag{1}$$

$$\mathbf{K} = \begin{bmatrix} k_1 & -k_1 & 0 \\ -k_1 & k_1 + k_2 & -k_2 \\ 0 & -k_2 & k_2 + k_3 \end{bmatrix}$$

$$y = \begin{bmatrix} y_1 \\ y_2 \\ y_3 \end{bmatrix}, \quad F = \begin{bmatrix} -F_c \\ 0 \\ F_0 \end{bmatrix} \tag{2}$$

y_1 y_3 respectively represents the displacement of the three mass of the pantograph; F_c and F_0 respectively represents the contact force of pantograph catenary and the lifting force of the pantograph.

2.3 Rigid Catenary Modeling

Based on beam theory, the vibration differential equation of AC rigid catenary is shown in (3).

$$EI\frac{\partial^4 y(x,t)}{\partial x^4} + \rho S\frac{\partial^2 y(x,t)}{\partial t^2} = F_c(x,t)\delta(x - x_t) \tag{3}$$

where, EI is the bending stiffness, ρ is the density, S is the transverse area, k_d is the stiffness, $F_c(x,t)$ is contact force of pantograph-AC rigid catenary, as shown in Fig. 3, establish the x-axis along the direction of the AC rigid catenary, establish y-axis vertically downwards, $y(x,t)$ represents the displacement in the y-axis direction at x, $\delta(x - x_j)$ is a dirac function

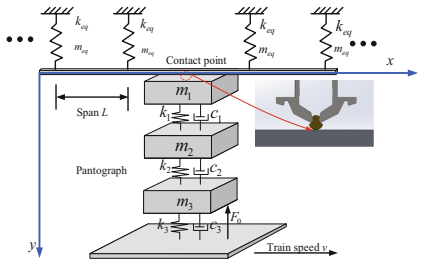

Fig. 3. Model of pantograph catenary

2.4 Double Pantograph Catenary Coupling Modeling

The dynamic equilibrium equation of double pantograph catenary model as follows:

$$\mathbf{M} \cdot \ddot{y} + \mathbf{C} \cdot \dot{y} + \mathbf{K} \cdot y = F \tag{4}$$

where, $\mathbf{M}$ is the mass matrix of the model, $\mathbf{C}$ is the damping matrix of the model, and $\mathbf{K}$ is the stiffness matrix of the model. y, $\dot{y}$, $\ddot{y}$ are the displacement vector and velocity vector, and acceleration vector of the model at the contact point, F is the load vector of the model at the contact point.

Figure 4 shows the model of a double pantograph catenary, and the contact force between the pantograph catenary calculated using the penalty function is shown in (5) and (6).

$$F_{ct}(t) = \begin{cases} k_c \triangle y_t(t) & \triangle y_t(t) > 0 \\ 0 & \triangle y_t(t) \leq 0 \end{cases} \tag{5}$$

$$F_{cl}(t) = \begin{cases} k_c \triangle y_l(t) & \triangle y_l(t) > 0 \\ 0 & \triangle y_l(t) \leq 0 \end{cases} \tag{6}$$

In (5) and (6), k_c is the coupling stiffness, and $\triangle y_l(t)$ is the displacement difference between the rigid catenary and the leading pantograph at time t; $\triangle y_t(t)$ is the displacement difference between the rigid catenary and the trailing pantograph at time t.

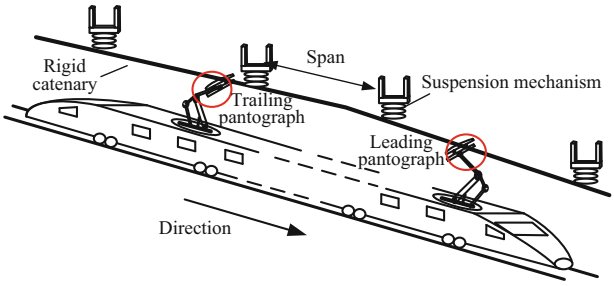

Fig. 4. Dual pantograph catenary model

3 Analysis of Structure

Through the analysis of the structure AC rigid contact network, the propagation of vibration waves in AC rigid catenary was analyzed.

3.1 Fluctuation Propagation of Rigid Catenary

According to the beam vibration differential equation and plane simple harmonic equation, the rigid catenary fluctuations velocity v_u as (7).

$$v_u = \frac{\pi}{L}\sqrt{\frac{EI}{\rho}} \tag{7}$$

From Fig. 5, it can be seen that as the span or unit density decreases, the fluctuations velocity gradually increases, and according to the actual operation of the train, the fluctuation speed is positively correlated with the train speed.

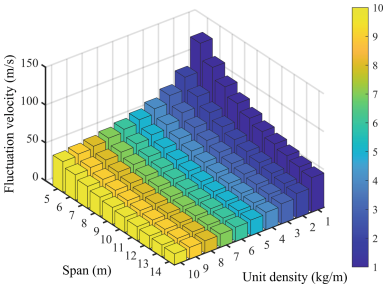

Fig. 5. The influence of structural parameters of rigid catenary on wave velocity

3.2 The Theoretical Value of the Span

The maximum theoretical value of the span can be as follows (8)

$$L^2 < \frac{768 \times 0.12 F_c EI}{4\pi^2 \rho m v^2} \tag{8}$$

Figure 6 can be obtained from (7), which shows the relationship between train speed and span, and it can be seen that the train speed increases with the decrease of span.

4 Simulation Result

The simulation model parameters refer to [11], and the simulation results at three different speed levels and three commonly used spans are shown in Fig. 7.

From Fig. 7, the fluctuation of contact force is the smallest at the span of 6m, followed by the span of 8m, and the largest at the span of 10m.

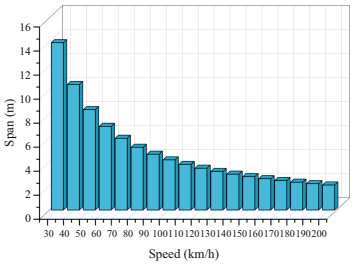

Fig. 6. The relationship between train speed and span

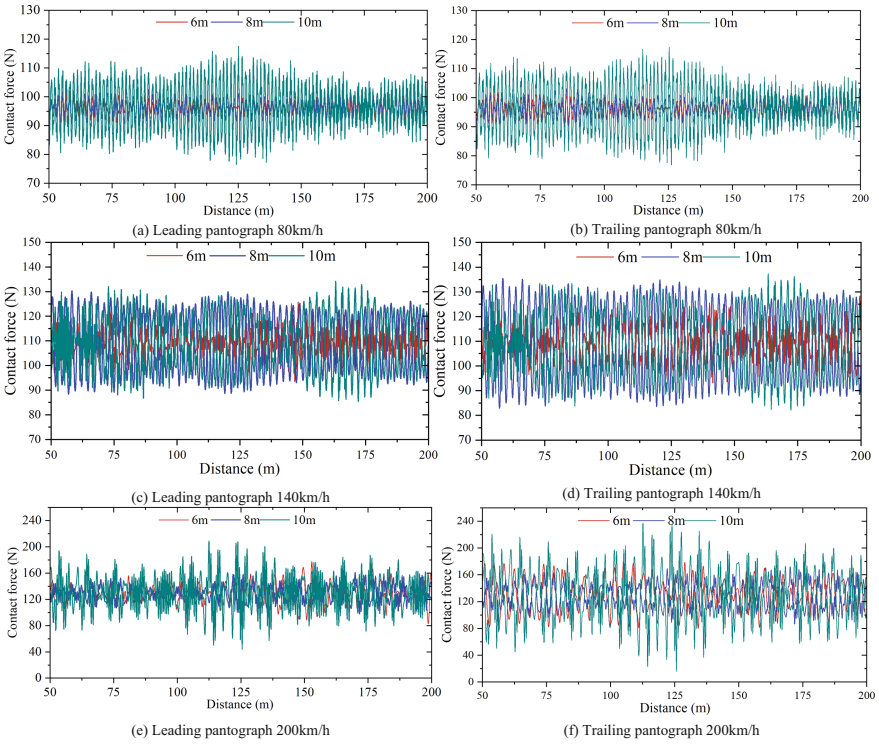

Fig. 7. Simulation data of AC rigid catenary under different speed levels and common spans

In addition, by comparing Fig. 7(a)–(f), it can be seen that when the span is the same, the fluctuation of simulation data increases with the train speed; At the same speed level, the fluctuation of simulation data increases with the span; At the same train speed and span, there is a significant fluctuation in the simulation data of the trailing pantograph.

In Fig. 8, the simulation data of the AC rigid catenary were analyzed, including median, lower quartile (Q1), upper quartile (Q3), interquartile spacing (IQR), lower edge, and upper edge. At train speeds of 80 km/h and 200 km/h, Q1–Q3 and 1.5 IQR with a span of 6 m are the narrowest, 8m is the narrower, and 10 m is the most dispersed.

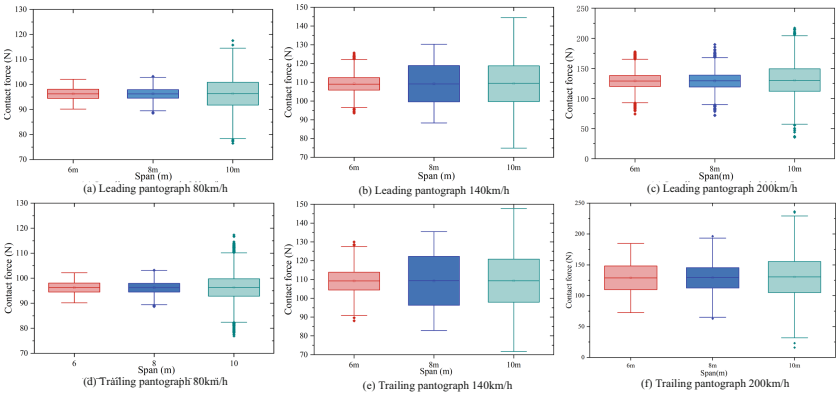

Fig. 8. Box-type diagram of simulation data under different speed levels and common spans

Especially at 140 km/h, the interquartile spacing Q1–Q3 and 1.5IQR between the dual pantographs are close.

In addition, the box-type diagram is symmetrical about its respective centerline, so the contact forces at different speed levels and commonly used spans roughly follow a normal distribution. At 80, 140, and 200 km/h, the average contact forces between the double pantograph and the AC rigid catenary are approximately 97N, 110N, and 130N, respectively. Therefore, among commonly used spans, a span of 8 or 10 m is suitable for train speeds below 80 km/h, while a span of 6 or 8 m is suitable for train speeds between 80 and 140 km/h.

5 Conclusion

In this paper, establishes a dual pantograph-catenary coupling model for rigid catenary, analyzes the structure of AC rigid catenary, and simulates contact forces at different speed levels and common spans.

1. Through the analysis of the structure of AC rigid catenary, it can be seen that as the span or unit density decreases, the fluctuation speed gradually increases. And the train speed is negatively correlated with the span value.
2. Through simulation analysis, among commonly used spans, the span of 8 or 10 m is suitable for train speeds below 80 km/h, while the span of 6 or 8 m is suitable for train speeds between 80 and 140 km/h.

Acknowledgments. This research is supported by National Natural Science Foundation of China Regional under Grant (Grant No. 52067013), Natural Science Key Foundation of Gansu Provincial Department of Science and Technology under Grant (Grant No. 21JR7RA280), Natural Science Key Foundation of Gansu Provincial Department of Science and Technology under Grant (Grant No. 22JR5RA318), and Natural Science Foundation of Gansu Provincial Department of Science and Technology under Grant (Grant No. 22JR11RA162).

References

1. Bruni, S., Bucca, G., Carnevale, M., Collina, A., Facchinetti, A.: Pantograph–catenary interaction: recent achievements and future research challenges. Int. J. Rail Transp. **06**(02), 57–82 (2018)
2. Chen, X., Zhang, X., Wang, Y., Wang, X.: Improved study on the fluctuation velocity of high-speed railway catenary considering the influence of accessory parts. IEEE Access **08**(02), 138710–138718 (2020)
3. Song, Y., Wang, H., Liu, Z.: An investigation on the current collection quality of railway pantograph-catenary systems with contact wire wear degradations. IEEE Trans. Instrum. Meas. **70**(23), 1–11 (2021)
4. Song, Y., Wang, Z., Liu, Z., Wang, R.: A spatial coupling model to study dynamic performance of pantograph-catenary with vehicletrack excitation. Mech. Syst. Signal Process. **151**(11), 107336–107387 (2021)
5. Wang, S., Li, X.: Vibration characteristics analysis and structure optimization of catenary portal structure on four-wire bridge. Struct. Durab. Health Monit. **16**(04), 361–382 (2022)
6. Yan, N.: Analysis of rigid suspension catenary system and its application prospect. Electrified Railw. **33**(05), 64–67 (2022). (in Chinese)
7. Chen, L., Duan, F., Song, Y.: Assessment of dynamic interaction performance of high-speed pantograph and overhead conductor rail system. IEEE Trans. Instrum. Meas. **08**(71), 1–14 (2021)
8. Benet, J., Femando, C., Tomas, R., Pedro, T., Enrique, A.: A dynamic model for the study and simulation of the pantograph-rigid catenary interaction with an overlapping span. Appl. Sci. **11**(16), 7445–7470 (2021)
9. Bautista, A., Montesinos, J., Pintado P.: Dynamic interaction between pantograph and rigid overhead lines using a coupled FEM-multibody procedure. Mech. Mach. Theory **97**(03), 100–111 (2016)
10. Simarro, M., Postigo, S., Cabrera, J., Castillo, J.: A procedure for validating rigid catenary models using evolutionary techniques. Comput. Struct. **228**(11), 106145–106165 (2020)
11. Guan, J., Wu, J.: Dynamic coupling equations between pantograph and overhead rigid conductor rail by using numerical method. J. Railw. Sci. Eng. **13**(02), 362–368 (2016). (in Chinese)